Schlieren visualization of focused ultrasound beam steering for spatially specific stimulation of the vagus nerve

Kawasaki, S.; Dijkema, E.; Saccher, M.; Giagka, Vasiliki; Schleipen, J.J.H.B.; Dekker, R.

Citation (APA)
Kawasaki, S., Dijkema, E., Saccher, M., Giagka, V., Schleipen, J. J. H. B., & Dekker, R. (2021). Schlieren visualization of focused ultrasound beam steering for spatially specific stimulation of the vagus nerve. In *2021 10th International IEEE/EMBS Conference on Neural Engineering (NER)* (pp. 1113-1116). Article 9441225 IEEE. https://doi.org/10.1109/NER49283.2021.9441225

Important note
To cite this publication, please use the final published version (if applicable).
Please check the document version above.

Schlieren visualization of focused ultrasound beam steering for spatially specific stimulation of the vagus nerve

S. Kawasaki, E. Dijkema, M. Saccher, V. Giagka, J.J.H.B. Schleipen and R. Dekker

Abstract— In the bioelectronic medicine field, vagus nerve stimulation (VNS) is a promising technique that is expected to treat numerous inflammatory conditions, in addition to the currently FDA approved treatment for epilepsy, depression and obesity [1]. However, current VNS techniques are still limited in the spatial resolution that they can achieve, which limits its therapeutic effect and induces side effects such as coughing, headache and throat pain.

In our prior work, we presented a curved ultrasound (US) transducer array with a diameter of 2 mm and with 112 miniature US transducer elements, small enough to be wrapped around the vagus nerve for precise ultrasound nerve stimulation [2]. Due to the curved alignment of the US transducers with 48 of the elements simultaneously excited, the emitted US was naturally focused at the center of the curvature. Building on this work, we employ a beam steering technique to move the focal spot to arbitrary locations within the focal plane of the transducer array. The beam steering was controlled through an in-house built US driver system and was visualized using a pulsed laser schlieren system. The propagation of the US pulse in water was imaged and recorded. This method was found to be a rapid and effective means of visualizing the US propagation.

I. INTRODUCTION

Vagus nerve is the tenth cranial nerve and has projections to many of the visceral organs. It serves as a bidirectional link between the brain and the body. Currently FDA approved vagus nerve stimulators are used to treat depression, epilepsy, cluster headache and obesity. Recent developments in the bioelectronic medicine field have shown that vagus nerve stimulation (VNS) is also effective in treating inflammatory related diseases such as rheumatoid arthritis, and inflammatory bowel disease by decreasing the production of pro-inflammatory cytokines such as TNFα [1]. However, VNS suffers from side effects such as coughing, headache and throat pain due to its off-target stimulation. Thus, a stimulation technique with higher specificity is needed [3].

From a device fabrication perspective, researchers have worked on cuff electrodes with multiple channels to accurately localize the electrical current to achieve higher specificity [4]. However, this remains to be a challenge since the thicker myelinated A fibers tend to be stimulated an order of magnitude more easily than the thinner unmyelinated C fibers. To further increase the stimulation specificity, A. Ghazavi et al. created 20 μm wide shank-structures which have multiple electrodes on the surface that can be pierced into the nerve to provide localized electrical stimulation [5]. Although this was successful in rodent models, it is still an open question whether such an invasive technique can be safely used for human vagus nerve stimulation in the long run.

By taking into account the anatomy of the vagus nerve, some researchers stimulated the vagus nerve at locations near the end organ where it is expected that the off-target effect can be reduced [6]. Unfortunately, at these deeper locations the implantation of devices is more difficult due to its limited space and lack of suitable anchor points. For a less invasive approach, V. Cotero et al. used ultrasound (US) stimulation to achieve stimulation of these nerves near the end organ. In their work, they applied transcutaneous low intensity US (290.4 mW/cm²) at the vagus nerve innervation within the spleen and modulated the anti-inflammatory pathway [7]. Furthermore, they showed that it is possible to achieve selectivity by stimulating the vagus nerve innervation within the liver to modulate the hepatic pathway. However, the direct consequence of stimulating the vagus nerve near the end organ, either electrically or ultrasonically, is that the simultaneous access to other vagus nerve branches becomes limited. For example, in case of electrical stimulators targeting different nerves, multiple implants are required, and for US stimulation, the US transducer outside of the body must be manually repositioned each time the targeted nerve is changed. Therefore, there is still a competing interest to keep the stimulus at the cervical level where all the nerve fibers are accessible.

In our prior work, we presented a highly miniaturized US cuff device [2]. This US cuff device is made of an array of 112 MEMS US transducer elements that is curved into a 2 mm diameter half cylinder. The acoustic frequency was 15 MHz to achieve high spatial resolution, and the US cuff was able to transmit a spatial peak average intensity (I_{SPPA}) of 3.2 W/cm². We hypothesized that such a device wrapped around the cervical vagus nerve can stimulate it at the neuronal to fascicular level.

In this paper, we demonstrate the US beam steering by using a custom-built 32-channel US driver system. For verifying the US field, an optical setup called the pulsed laser schlieren system was built to visualize the US propagation [8]. Schlieren optics is a useful tool to visualize the change in the refractive index in a transparent medium upon US propagation. This schlieren imaging technology has found a variety of applications for ballistics, air flows and acoustic waves visualizations, and this is the first time it is used in the US neuromodulation field. The advantage of using schlieren techniques in comparison to a hydrophone is that the US field

can be imaged simultaneously along with the US cuff device. Furthermore, the US field will not be altered by the hydrophone tip. Finally, it may allow opportunities to combine fluorescent imaging of action potentials with simultaneous US imaging.

II. MATERIALS AND METHODS

In this work, a Capacitive Micromachined Ultrasonic Transducer (CMUT) was used to generate the US. The CMUT device is a capacitor cell which consists of two circular flat electrodes separated by a vacuum gap. One of the electrodes is a fixed bottom membrane on a silicon substrate and the other electrode is a movable top membrane that is facing the medium. By applying an AC voltage at US frequencies, the electrical field actuates the top membrane and US is transmitted into the medium. The CMUT devices used in this research have a diameter of 25 µm, and 24 CMUT devices were connected in parallel to form a single line which will be referred to as a CMUT element. Figure 1 shows the US cuff assembled on a PCB. The US cuff has 112 CMUT elements aligned in a 2 mm diameter half circle. The CMUT elements are connected to the bondpad via aluminum interconnects encapsulated in polyimide. The bondpad region is connected to a PCB via wirebonding.
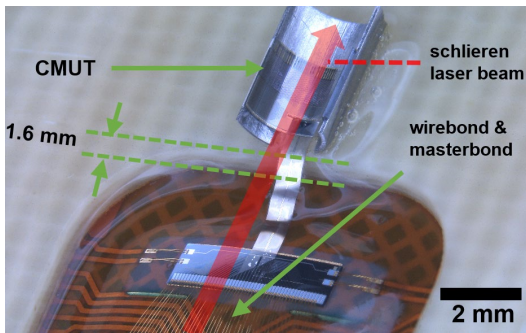

Fig. 1. CMUT sample that was used for the experiment. In order to have a clear optical path through the US field, the position of the bond pad was designed to be 1.6 mm lower than the position of the CMUT. This kept the added height of the wirebond and the masterbond to be slightly lower than the CMUT array.

A. Pulsed laser Schlieren System

Figure 2 shows the pulsed laser schlieren system. The light of a red laser diode (SANYO DL-6147-240) is focused onto a 20 µm diameter pinhole using a microscope lens for spatial filtering and subsequent aberration reduction. The diverging laser beam is collimated using a collimating lens with a focal length of 200 mm. Next, the parallel beam travels through the water tank, after which it is focused by a 200 mm focusing lens onto a 10 µm diameter chromium mirror, blocking the main non-aberrated laser beam. Therefore, in the initial state, the camera (uEYE), that is positioned behind the mirrorstop, will
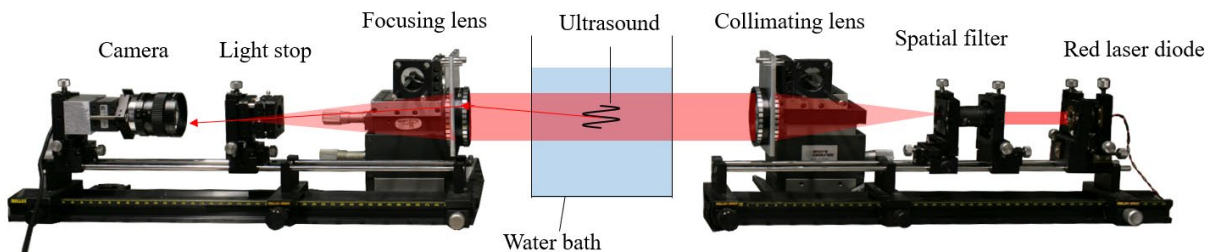
capture a pitch-black image. The combination of a camera objective lens and laser focusing lens provides a sharp image of the plane of US propagation onto the camera image sensor.

When a CMUT array is positioned within the water tank, the US field results in a modulation of the refractive index of water and diffracts part of the light to go beyond the obstructing mirror, which will subsequently be captured by the camera. An US signal with an acoustic frequency of 14.3 MHz was generated in bursts of 15 cycles at a pulse repetition frequency of 3 kHz. For each generated US burst, a waveform generator (Agilent 3295A) was triggered to generate a 100 ns pulse to drive the laser diode. The delay time between the US burst and the laser pulse was incrementally increased from 0 µs to 3.35 µs in 100 ns steps. Due to the stroboscopic effect, the camera visualizes the US as slowly moving waves through the water. The US and laser/imaging setup have been synchronized and controlled using Labview software. During the actual measurements the ambient room light was turned off.

To focus the US to a certain point within the curvature, beam steering was used. The appropriate time delay for each element was calculated as follows. The coordinate where we would like to focus is defined as $\mathbf{x}$. The distance from each transducer element to the $\mathbf{x}$ is D_i :

$$D_i = |\mathbf{x} - \mathbf{q}_i|, \qquad i \in [1, 32]$$

where, $\mathbf{q}_i$ is the coordinate of the individual 32 US transducer elements. The time delay (T_i) applied to each element is given by,

$$T_i = \frac{D_i - \min(D_i)}{v}, \qquad i \in [1, 32]$$

where, v is the speed of US in water. The calculated value is rounded to an integer multiple of 5 ns, which is the resolution of the US driver system. The US driver used for this work was an in-house built US driver system that is based on the HV7351 chips (Microchips).

B. Simulation with FOCUS

The experiment was simulated with the Fast Object-Oriented C++ US Simulator (FOCUS) [9]. In this simulation, 32 rectangular US transducer elements with a width of 25 µm and a length of 0.65 mm were arranged in a curved array like the experiment. The medium used for the simulation was water with a sound velocity of 1500 m/s. The US frequency was 14.3 MHz, the number of cycles was 15, and the velocity at which the US element vibrates was set to 1 m/s. The US field was simulated using frequency domain simulation assuming continuous wave of US with a phase delay. The intensity of the US field was given by, $I = P^2/Z_0$ where, I is the intensity of the US field, P is the acoustic pressure and Z_0

Fig. 2. Pulsed laser schlieren setup

1114

is the characteristic acoustic impedance of water which is 1.5 MRayl. All simulation results were normalized by dividing the US intensity by the maximum intensity within the same figure.

C. Hydrophone measurement

A fiber optic hydrophone (Precision Acoustics) was used to measure the US field. The tip of the hydrophone was scanned horizontally for 1.6 mm and vertically for 1 mm from the focal point. In total, 2091 measurements were taken for obtaining a single US field profile. Since each measurement at a certain coordinate took 6 seconds, the total time it took for obtaining a single image was 3.5 hours. The amplitude of the US signal used to drive the transducer elements had 35 V DC bias voltage and an additional 25 V amplitude square wave at 14.3 MHz.

III. RESULT

Figure 3 shows several raw images obtained from the camera. The semi-circular shape (red bold line) is where the US cuff was positioned. The triangular shadow on both sides of the US cuff is the epoxy that was used to glue the US cuff to the PCB. The 32 CMUT elements that were actively driven are circled with a dotted line. In the figure the US propagates upwards focusing in the center of the US cuff. When the active US elements were located near the center of the US cuff (top row in figure 3), the US field focused in an elongated shape with two prominent sidelobes. Meanwhile, when the active elements were located near the edge of the US cuff (bottom row in figure 3), the US field showed a clear interference pattern. In this case, the distance between two neighboring high intensity peaks at the center was measured to be 66 µm. This is nearly half the US wavelength of 52 µm, in correspondence with what is expected for an interfering wave. The small increase is due to the fact the US signals are slightly tilted upwards.

The advantage of using the schlieren method is the fast image acquisition speed. To demonstrate this, the focus location was varied to 100 locations and a video was taken sequentially one after another without any pause[1]. The total duration to take the video was only 5 minutes. It is possible to see that the video was taken in real time because particles floating in the liquid are moving continuously throughout the video.

In figure 4, a single frame from the schlieren image at 2.01 µs was converted to a heat map and was compared to the US field measured with a hydrophone. In the schlieren image to ignore excess noise floor, the normalized intensity beneath 0.7 was removed. In both the schlieren image and the hydrophone measurement we see that the intensity of the left sidelobe is slightly higher than the intensity of the right sidelobe. This is due to the imperfect alignment of the transducers array during the assembly process. Even with this rough image quality the similarity between the hydrophone measurement and the US visualization confirms that schlieren imaging can be successfully used for fast US visualization.

To improve the image quality, another video was taken with 34 ns time intervals between each image. The increased number of frames helped to decrease the noise from dust particles. A background subtraction technique was used to remove the static parts of the image, such as scratches, and shadows from the glue and the US cuff. Next, the intensity profile of the US field was extracted by integrating it over the entire US propagation. Figure 5 shows the result of the simulation on the left and the integrated schlieren image on the right. In order to facilitate the comparison between these images, the images were cropped to the same size and aspect ratio. In all images the US cuff is represented by a white line. Clearly the direction of the US matches very well the simulated results. We also see that as the US focus is further from the US transducers, the US lobe size increases which is consistent with the simulation result.

The peak negative acoustic pressure measured at the center of the focus was 1.7 MPa. The spatial peak temporal average intensity that could currently be achieved with the US driver system was 6.5 W/cm^2 with 90 kHz pulse repetition frequency and 15 cycles per each burst. The mechanical index was 1.4 which is lower than the limit defined for US imaging applications by the FDA (<1.9). At the moment, we believe that this intensity should be sufficient to stimulate the nerve according to prior work [7]. However, it is still not clear since the higher acoustic frequency will likely have a higher stimulation threshold levels to stimulate the neurons.
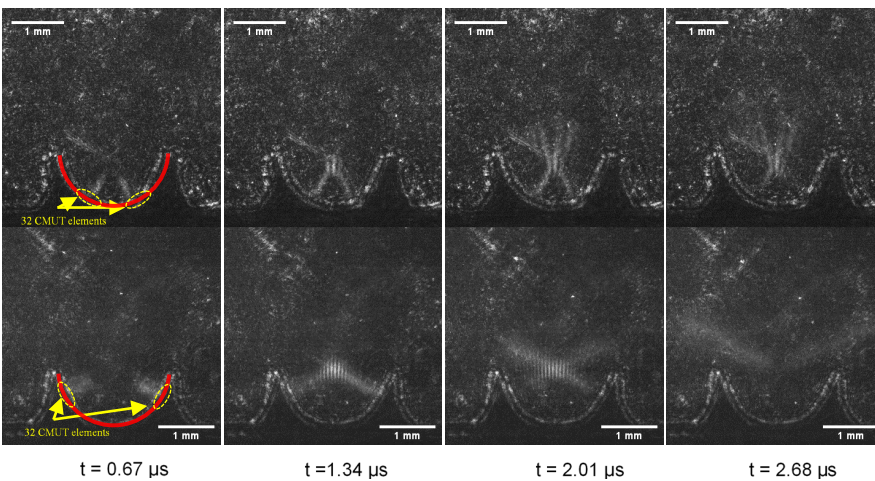

t = 0.67 µs   t = 1.34 µs   t = 2.01 µs   t = 2.68 µs

Fig. 3. Snap shots of the US schlieren movie from left to right with the 32 US elements near the center (top row) and 32 US transducers near the edge (bottom row)
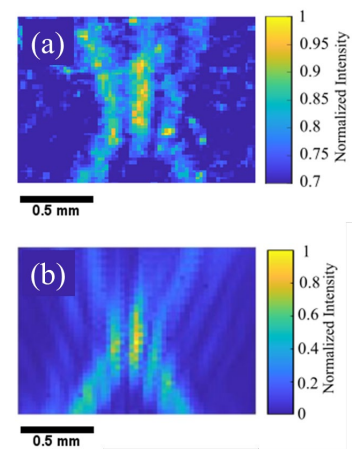
Fig. 4. (a) Schlieren image intensity profile and (b) hydrophone measured intensity profile
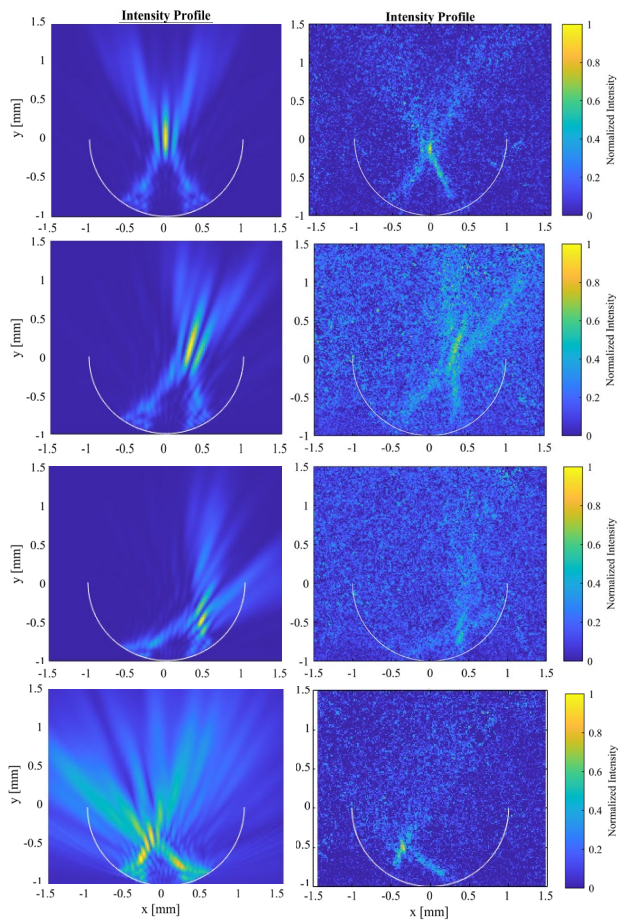
Fig. 5. US field comparison between simulation (left) and schlieren (right)

IV. Discussion and Conclusion

In this work, beam steering of the ultrasonic field produced by an US cuff was demonstrated using the pulsed laser schlieren setup. Schlieren imaging allowed faster US visualization (few minutes) compared to hydrophone measurement (few hours). In addition, once the system is up and running it took less time to observe the US field even compared to simulating it with FOCUS where it took tens of seconds to simulate a single frame with enough resolution.

However, schlieren imaging does not produce an absolute measurement of the US field, so it should be used as a complementary technique to hydrophone measurements. Yet it is possible to calibrate the system for a limited range of pressures [10]. For calibration, the key parameters that need to be determined are the exposure time, the pulse repetition frequency and the laser intensity. Although a wide range of US intensity could be visualized, the dynamic range for a specifically calibrated range, spans to only one order of magnitude as shown in the linear scale used in Figure 4 and 5. Finally, due to the optics that it requires, it would not be feasible to integrate this technology for in-vivo experiments. Meanwhile, experiment which are done in an ex-vivo setup may allow for the schlieren setup to be integrated.

In conclusion, further miniaturized US transducers with varying size and shapes will be available in the future. This will increase the complexity of the ultrasound field that will be used for US neuromodulation. Thus, visualizing the relative intensity of the US field with a schlieren setup would give an intuitive feedback to check if the US system is working properly. This would clarify a lot of the ambiguity within the works that are done in US neuromodulation and greatly facilitate the research in this field.

References

[1] C. M. Noller, Y. A. Levine, T. M. Urakov, and J. P. Aronson, "Vagus Nerve Stimulation in Rodent Models : An Overview of Technical Considerations," vol. 13, no. September, pp. 1–11, 2019, doi: 10.3389/fnins.2019.00911.

[2] S. Kawasaki *et al.*, "Pressure measurement of geometrically curved ultrasound transducer array for spatially specific stimulation of the vagus nerve," *Int. IEEE/EMBS Conf. Neural Eng. NER*, vol. 2019-March, pp. 1239–1242, 2019, doi: 10.1109/NER.2019.8717064.

[3] V. Giagka and W. A. Serdijn, "Realizing flexible bioelectronic medicines for accessing the peripheral nerves – technology considerations," *Bioelectron. Med.*, vol. 4, no. 1, pp. 1–10, 2018, doi: 10.1186/s42234-018-0010-y.

[4] M. Dali *et al.*, "Model based optimal multipolar stimulation without a priori knowledge of nerve structure: Application to vagus nerve stimulation," *J. Neural Eng.*, vol. 15, no. 4, 2018, doi: 10.1088/1741-2552/aabeb9.

[5] M. I. Romero-ortega, A. Ghazavi, M. A. Gonz, and S. F. Cogan, "Intraneural ultramicroelectrode arrays for function-specific interfacing to the vagus nerve," vol. 170, no. September, 2020.

[6] S. C. Payne *et al.*, "Anti-inflammatory effects of abdominal vagus nerve stimulation on experimental intestinal inflammation," *Front. Neurosci.*, vol. 13, no. MAY, pp. 1–15, 2019, doi: 10.3389/fnins.2019.00418.

[7] V. Cotero *et al.*, "Noninvasive sub-organ ultrasound stimulation for targeted neuromodulation," *Nat. Commun.*, no. 2019, pp. 1–12, doi: 10.1038/s41467-019-08750-9.

[8] T. Neumann and H. Ermert, "A New designed Schlieren System for the Visualization of Ultrasonic Pulsed Wave Fields with High Spatial and Temporal Resolution," *2006 IEEE Ultrason. Symp.*, pp. 244–247, 2006, doi: 10.1109/ULTSYM.2006.74.

[9] D. Chen, J. F. Kelly, and R. J. McGough, "A fast near-field method for calculations of time-harmonic and transient pressures produced by triangular pistons," *J. Acoust. Soc. Am.*, vol. 120, no. 5, pp. 2450–2459, 2006, doi: 10.1121/1.2356839.

[10] H. A and C. I. Zanelli, "Quantitative real-time pulsed schlieren imaging," *Ultrason. Symp.*, pp. 1223–1228, 1991.